Obrabotka metallov (tekhnologiya, oborudovanie, instrumenty) = Metal Working and Material Science. 2023 vol. 25 no. 2 pp. 17–31
ISSN: 1994-6309 (print) / 2541-819X (online)
DOI: 10.17212/1994-6309-2023-25.2-17-31

NSTU NETI

Obrabotka metallov - Metal Working and Material Science

Journal homepage: http://journals.nstu.ru/obrabotka_metallov

Analytical model of equal-channel angular pressing of titanium sponge

Ivan Berezin [1, 2 a,*], *Alexander Zalazinsky* [3, b], *Denis Kryuchkov* [3, c*]

[1] Ural Federal University named after the first President of Russia B.N. Yeltsin, 19 Mira st., Ekaterinburg, 620002, Russian Federation
[2] GUIDE SYSTEMS LLC, 18b Rodonitova str., Ekaterinburg, 620089, Russian Federation
[3] Institute of Engineering Science, Ural Branch of the Russian Academy of Science, 34 Komsomolskaya str., Ekaterinburg, 620049, Russian Federation

[a] https://orcid.org/0000-0002-8674-3352, i.m.berezin@urfu.ru, [b] https://orcid.org/0000-0001-8352-5475, zalaz@list.ru,
[c] https://orcid.org/0000-0001-8585-3544, kru4koff@bk.ru

ARTICLE INFO

Article history:
Received: 28 February 2023
Revised: 29 March 2023
Accepted: 28 April 2023
Available online: 15 June 2023

Keywords:
Model
Equal-channel angular pressing
Titanium sponge
FEM

Funding
The work was financed by the State budget. A theme No. 0391-2019-0005 "Development of scientific bases of designing of optimum production engineering plastic forming of metal materials with the secured level of a continuity and physicomechanical properties".

Acknowledgements
Researches were conducted at core facility of NSTU "Structure, mechanical and physical properties of materials".

ABSTRACT

Introduction. The use of equal-channel angular pressing (*ECAP*) of metal powder makes it possible to obtain practically non-porous blanks with high hardness, with a high level of accumulated deformation and with the formation of an ultra-fine-grained structure. A relevant issue for the study of the semi-continuous *ECAP* process remains a reliable assessment of the energy-power parameters of the process and the prediction of the porosity of compressed materials. This, in turn, is due to the need to develop sufficiently accurate, reliable and simple mathematical models for practical application. **The purpose of the work** is to develop an analytical model of the process of equal-channel angular pressing of porous material. Powdered screening of spongy titanium of the *TG-100* brand was selected as a model of the material for the study. The object of the study is the process of semi-continuous equal-channel angular pressing of axisymmetric porous briquette of titanium sponge in the channel of the mold. It is assumed that the *ECAP* uses a punch to create back pressure. For the solution, a process scheme, a statically permissible load scheme on a layer of intense deformation and a kinematically permissible flow scheme of a plastically compressible medium in a layer **are determined**. A system of equations is constructed in accordance with the accepted schemes. The equation power balance is applied. The analytical equation is solved by the method of successive approximations. Finite element simulation of the porous titanium *ECAP* process was carried out at the angles of intersection of the mold channels at 45°, 50°, 55° and 60°. **Results and Discussion.** The porosity of the blank is determined at different stages of the *ECAP* process. A diagram of the change in pressure on the punch using the analytical solution and finite element simulation is obtained. It is revealed that the results of the analytical solution are consistent with the data of the finite element simulation. The highest stress level occurs in the process of equal-channel angular pressing at α = 45°, however, the distribution of relative density over the cross section is most uniform. The maximum value of the pressure on the working punch decreases with an increase in the angle α. Rational technological parameters of pressing porous blanks should provide the maximum permissible pressure on the deforming tool. From this condition, in each specific *ECAP* process, it is possible to determine the optimal angle value from the analytical solution.

For citation: Berezin I.M., Zalazinsky A.G., Kryuchkov D.I. Analytical model of equal-channel angular pressing of titanium sponge. *Obrabotka metallov (tekhnologiya, oborudovanie, instrumenty) = Metal Working and Material Science*, 2023, vol. 25, no. 2, pp. 17–31. DOI: 10.17212/1994-6309-2023-25.2-17-31. (In Russian).

Introduction

The essence of the severe plastic deformation (*SPD*) process is pressure shaping, carried out at temperatures below the recrystallization threshold of the deformed material, with a high level of cumulative deformation and leading to the formation of ultrafine-grained structures in metals. Quite a few methods

*** Corresponding author**
Kryuchkov Denis I., Ph.D. (Engineering), Researcher
Institute of Engineering Science,
Ural Branch of the Russian Academy of Science,
34 Komsomolskaya str.,
620049, Ekaterinburg, Russian Federation
Tel.: 8 (343) 374-50-51, **e-mail:** kru4koff@bk.ru

of *SPD* are known: high-pressure torsion [1], pack rolling [2], all-round forging [3], cyclic extrusion and compression, also called “hourglass pressing” [4], equal-channel angular pressing [5] and others. A detailed review of SPD methods was performed by *R.Z. Valieev* et al. [6] and *V.M. Segal* [7]. The desire to improve the performance of *SPD* processes has stimulated the development of various methods of continuous pressing. The methods of continuous pressing, which have found the widest application in industry, include conformal (forming of long-rolled metal by the method of continuous extrusion), Linex [8], and combined rolling-pressing [8–9]. The work of *V.M. Segal* [10] considered the theoretical aspects of the process that combines the methods of equal-channel angular pressing and conformals.

SPD of powder and porous materials realizes a complex stress-strain state characterized by joint triaxial compression and shear [11]. The process of consolidation from pure aluminum powder by the method of equal-channel angular pressing with torsion is described in [5], where it is shown that reiteration of *SPD* makes it possible to accumulate structural changes in the material. This contributes to a more efficient closure of large structural defects, and also increases the number and size of areas of mechanical adhesion of particles due to the initiating effect of shear deformation. It was shown in [12] that *SPD* for porous titanium and a porous titanium-magnesium composite makes it possible to obtain an ultrafine-grained structure and good contact between particles.

Of particular interest is the method of *equal-channel angular pressing* (*ECAP*) of powder and porous materials. It was shown in [13] that the use of *ECAP* of a metal powder makes it possible to obtain practically pore-free blanks with high hardness even after a single pressing. However, a particularly important advantage of *ECAP* is the possibility of consolidating powder and porous materials at lower temperatures compared to the temperature required in traditional powder metallurgy methods [14].

At the same time, it is of great practical interest to obtain semi-finished products from powdered raw materials of hard-to-deform and low-plastic alloys and metals, such as titanium, with uniform properties and minimal porosity. The reduction in the cost of titanium powder products directly depends on the reduction in the cost of production methods and pressure shaping of titanium powders. Of great interest are methods for the production of titanium powder, close in its physical and mechanical properties and morphology of individual particles to titanium sponge obtained by the traditional *Kroll* method. *International Titanium Powder, L.C.C.* (*Cristal US Inc., USA*) has developed a process for obtaining titanium powder (*Armstrong process*), suitable for the manufacture of essential components by powder metallurgy. *Chen et al.* [15] studied the process of cold compaction of Armstrong powders of the *Ti-6Al-4V* system. According to the data given in [16], this technology makes it possible to reduce the cost of manufacturing finished titanium products by at least two times. The authors of [17] presented an electrochemical method (*Cambridge process*) for the direct reduction of solid TiO_2. The *Rapid Plasma Quenching Process* (*Idaho Titanium Technologies, USA*) is based on the use of high-temperature plasma energy and makes it possible to reduce the cost of high-quality titanium powders’ production [18]. In [19], a method for obtaining cheap titanium powder from a titanium sponge using the technology of self-propagating high-temperature synthesis (*SHS*) is proposed. The use of *severe plastic deformation methods* for these materials will make it possible to obtain high-density blanks without the use of traditional energy- and labor-intensive titanium production technology.

It is worth noting that finely divided titanium sponge and powder compositions based on it are promising materials for the manufacturing powdered titanium products, which require high corrosion resistance, low weight and satisfactory strength properties at a low cost of raw materials. *NORSK Titanium* (*Norway*) has received two patents for the production of welding wire directly from titanium sponge (Patent *WO2011049465*, Patent *WO2012127426*). In [20], the effect of combined treatment, including hydrogenation/hydrogen removal and rolling, on the structure and mechanical properties of sponge titanium plates pressed by a shock wave was studied. The authors of [21] showed the possibility of using a porous material based on titanium sponge granules in the production of implants for osseointegration. In [22], the process of uniaxial pressing of titanium sponge powder was investigated. In [23–25], the effect of hydrogen doping on the properties of briquettes made of sponge titanium by pressing was investigated.

A variety of technologies for obtaining semi-finished products and rheological features of powdered titanium leads to the need for preliminary calculations to develop specific technical devices for its implementation. Reliable estimation of the energy-power parameters of the process and prediction of the porosity of pressed materials remains an important issue for the study of the *ECAP* semicontinuous process up to now. This in turn is associated with the need to develop sufficiently accurate, reliable, and simple for practical application mathematical models.

The **work aims to** develop a model of the process of semicontinuous *ECAP* of titanium-containing raw materials to improve the technological processes of manufacturing blanks and products.

To achieve this aim, it is necessary to determine the scheme of *ECAP*, a statistically admissible loading scheme for a severely deformed layer, and a kinematically admissible flow scheme for a plastically compressible medium in the layer, construct a system of equations, and compare the solution obtained with the developed system of equations with the finite element solution.

Materials and methods

The object of the study is the process of semicontinuous *ECAP* of an axisymmetric porous briquette (ϑ_b – initial porosity) of titanium sponge in the channel of the mold, which has an input part *6* and, crossing it at an angle 2α, output part *5* (fig. 1). The length of the briquette in the inlet and outlet parts of the channel at the current time are L_1 and L_2, respectively; L_b – the original length of the briquette, *dl* – the movement of the working plunger *1*; *D* – the diameter of the channel. Plunger *1* creates pressure P_1 on the briquette. The device also contains a plunger *2* to create counter-pressure (pressure P_2 that prevents the flow of the deformed material from the mold channel). Plunger 2 is used in the first pressing cycle. In the second and subsequent cycles, the backpressure creates the discard *4* of the previous cycle. The flow of the deformed material in the mold channel is prevented by frictional forces on the surface of the extruded blank.

Angular pressing provides severe plastic shear deformations in a thin layer located in the vicinity of section A–B (fig. 1) and separating the inlet ***I*** and outlet ***II*** parts of the mold channel. In this case, as a result of triaxial compression and intense shear deformation in layer A–B, the porosity of the titanium sponge decreases. In the input part *6* of the mold, the deformable material experiences a stressed state, similar to the usual pressing of a plastically compressible mass in a closed mold [26, 27].

Powdered sponge titanium of the *TG-100* grade (composition complies with *GOST 17747-79*) (fig. 2) without additional processing (sieving, secondary fine dividing, purification, etc.) was used as a material for the study. It was assumed that the titanium sponge material was pre-compacted by double-sided pressing to briquettes with a relative porosity of $\vartheta_b = 0.4$. The briquette material was considered to be homogeneous from the statistical viewpoint.

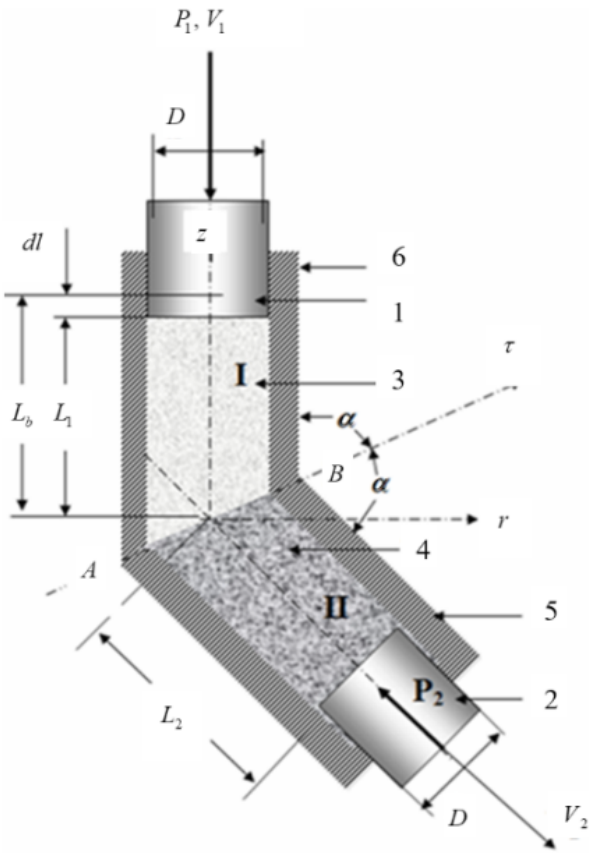

Fig. 1. Scheme of equal-channel angular pressing: *1* – punch creating working pressure; *2* – punch for back pressure; *3* – part of the extruded blank; *4* – pressed part of the blank; *5*, *6* – parts of the a pressing tool with output II and input I channels

Results and discussion

Each *ECAP* cycle has two stages. In the first stage, the material to be processed in part ***II*** of the mold channel is not deformed; in part ***I***, uniaxial compression of the porous mass takes place. Movement *dl* of plunger *1* leads to the

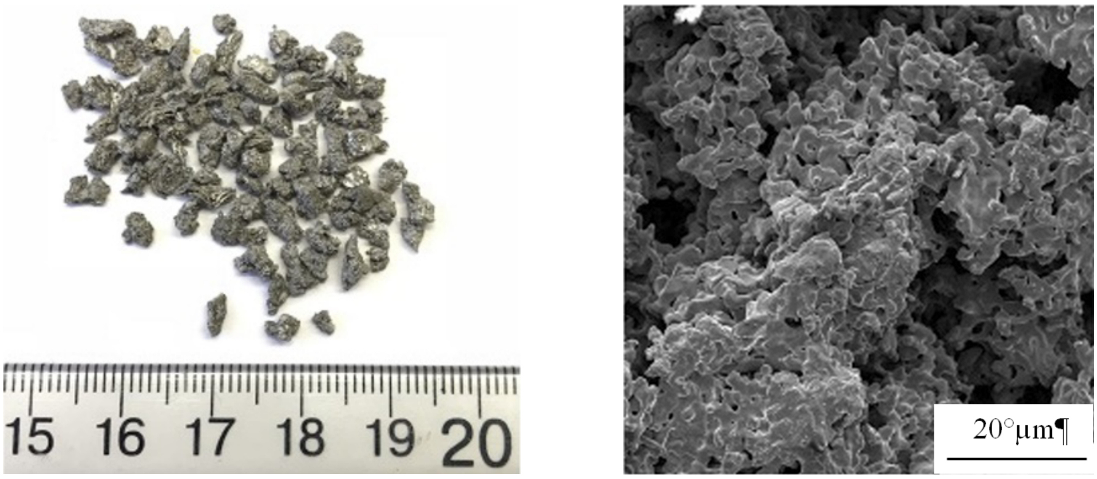

a *b*

Fig. 2. Titanium sponge (*a*); particle morphology (*b*)

occurrence and growth of the pressing force P_1, which reaches a certain maximum value P_1^* corresponding to the general flow of the deformed material in the mold channel. The action of contact friction in the mold leads to a decrease in pressure in the compressible particles as they move along the flow lines. In this case, the greatest pressure is experienced by particles located in the immediate vicinity of the working plunger; porosity reduction is possible according to the applied forces. In the second stage of the process, the pressed material flows out of the mold channel. In the section A-B, separating parts *6* and *5* of the mold, there is a force P_2^n that creates a counter-pressure to the flow of the plastic compressible medium (fig. 3, *a*).

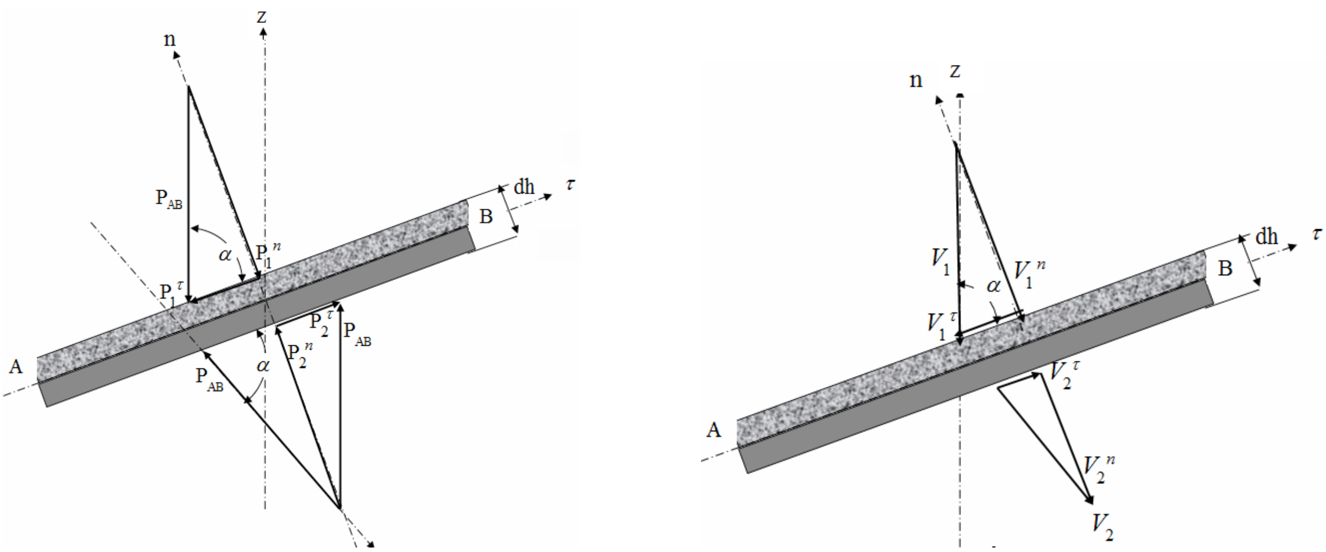

a *b*

Fig. 3. A statically permissible scheme of loading on a layer of severe deformation (*a*) and a kinematically permissible flow scheme of a plastically compressible medium in a layer A–B (*b*)

The force P_{AB} is determined by the equilibrium conditions of the forces acting on the compressible material in the mold channel:

$$P_{AB} = P_2 + \pi\tau_{c2} D L_2, \tag{1}$$

where P_2 is the force that creates counter-pressure; T_{c2} is a sliding friction stress on the mold surface; L_2 is the discard length; D is the channel diameter.

The power balance equation was applied to determine the power parameters of the second stage of the ECAP process:

$$P_1V_1 - P_2V_2 = \pi D(\tau_{c1}L_1V_1 + \tau_{c2}L_2V_2) + W\ |AB, \tag{2}$$

where V1, V2 are flow velocities of plastically compressible mass from mold channels ***I*** and ***II***; $W \mid AB$ is a power dissipation in the severe deformation layer (layer thickness $\Delta h \to 0$).

The physical equations of a representative element of the volume of a plastically compressible medium [28–30] have the form:

$$\sigma_{ij} = \sigma + 2\frac{T(\vartheta)}{H}\left(\xi_{ij} - \frac{1}{3}\xi\delta_{ij}\right) \tag{3}$$

where σ_{ij}, ξ_{ij} are components of the stress tensor and deformation rate tensor; σ ia an average normal stress; ξ is a volume strain rate; *T* is a shear stress intensity; *H* is a shear strain rate intensity; δ_{ij} is a *Kronecker* symbol.

The yield strengths in shear τ_s^* and isostatic compression p_s^*, depending on the relative porosity of the deformable medium, are given by the relations:

$$\tau_s^* = T = \tau_s(1 - \vartheta^{2/3}); \quad p_s^* = -\sigma = -\frac{2}{\sqrt{3}}\tau_s \ln\vartheta, \tag{4}$$

where τ_s is a shear yield strength of titanium particles; ϑ is a relative porosity of the titanium sponge volume element.

The dependencies $\tau_s^* / \tau_s = f_\tau(\vartheta)$ and $p_s^* / \tau_s = f_p(\vartheta)$ are shown in fig. 4.

Consider the stage of the *ECAP* process in which briquette compression is carried out similar to the compression of a porous mass in a closed mold, using the results of [31]. For the first approximation, it is assumed that external friction can be neglected; the motion of plunger *2* is given; the pressure on the plunger is determined from the power balance equation (2); at the initial moment of pressing, the porosity of the briquette material is equal to ϑ_b.

The boundary conditions in the cylindrical coordinate system (*r*, ϕ, *z*) have the following form: $\sigma_{rz}|r = R = 0$, $R = D/2$; $\nu_r|r = 0 = \nu_r|r = R = 0$, $\nu_z|z = 0 = 0$, $\nu_z|z = L_1 = V_1 = dl/dt$. For these conditions, the kinematically permissible velocity field is $\nu_r = 0$, $\nu_z = V_1 \cdot z/L_1$; components of the strain rate tensor: $\xi_{ij} = 0$, except $\xi_{zz} = -V_1/L_1$; the rate of volume change in part ***I*** of the mold channel $\xi = \xi_{ij}$. The degree of shear deformation Λ and the degree of volumetric deformation ε are of the form:

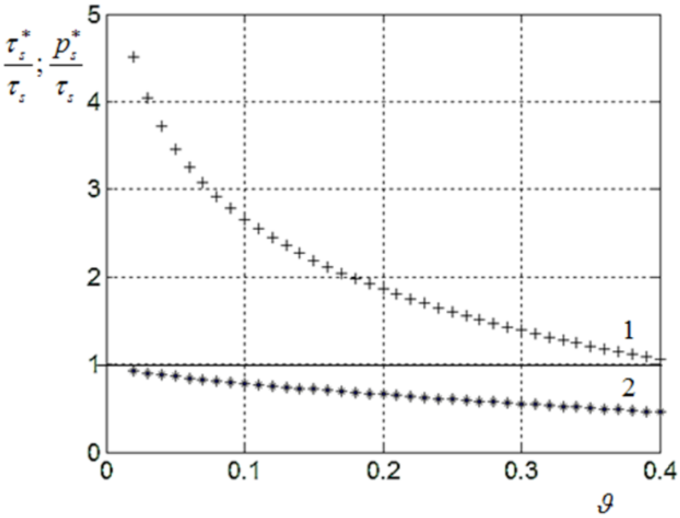

Fig. 4. Dependence of the yield strength of the compressible medium on porosity ϑ:
for isostatic compression $p_s^* / \tau_s = f_p(\vartheta)$ (*1*); for shear $\tau_s^* / \tau_s = f_\tau(\vartheta)$ (*2*)

$$\Lambda = \frac{2}{\sqrt{3}}\ln\left(\frac{L_b}{L_1}\right), \quad \varepsilon = \ln\left(\frac{L_1}{L_b}\right). \tag{5}$$

The values of the relative porosity ϑ_1 of the compressible medium in part ***I*** of the mold channel are the function of the movement *dl* of the working plunger:

$$\vartheta_1 = 1 - \frac{1 - \vartheta_b}{1 - dl / L_b}. \qquad (6)$$

Moving the tool in the first stage of the *ECAP* process is only possible when the pore volume is reduced. At the same time, p_s^* and the relative density of the compressible porous mass increase.

The dependence of the porosity ϑ on a load $\bar{p} = p_z / \tau_s$ of the plastic flow of the compressible medium is represented as follows:

$$\vartheta = (1 + \bar{p}^{3/2})^{-1}. \qquad (7)$$

Solving equations (6) and (7) made it possible to determine the change in the porosity of the titanium sponge and specific pressure as a function of plunger movement (fig. 5).

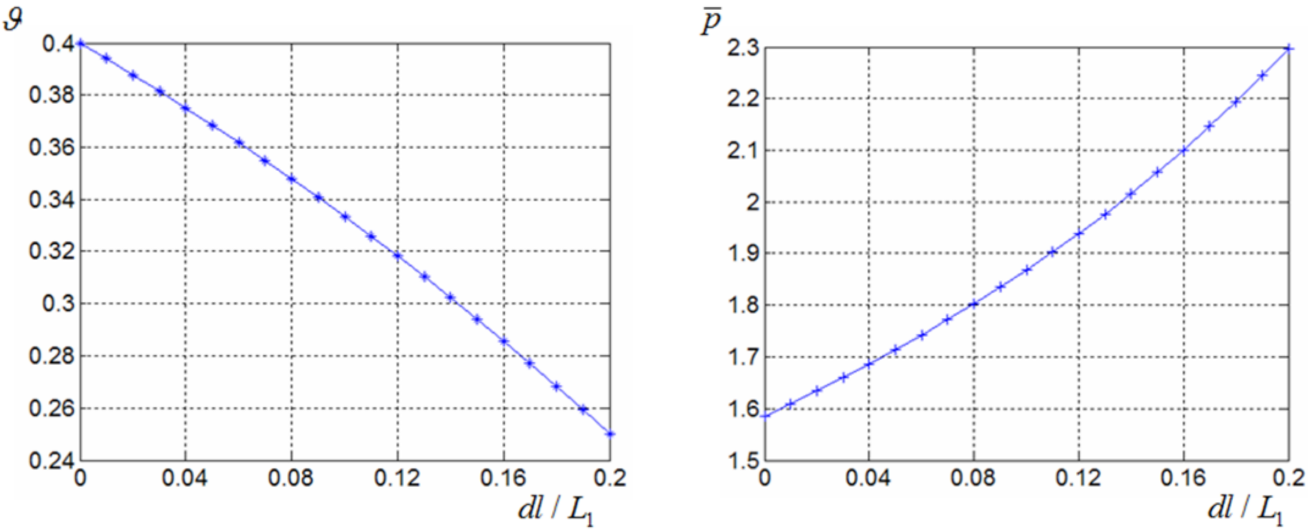

a *b*

Fig. 5. Change in the porosity ϑ of the compressible medium (*a*) and the specific pressure $\bar{p}$ (*b*) on the working plunger displacement dl/L_b.

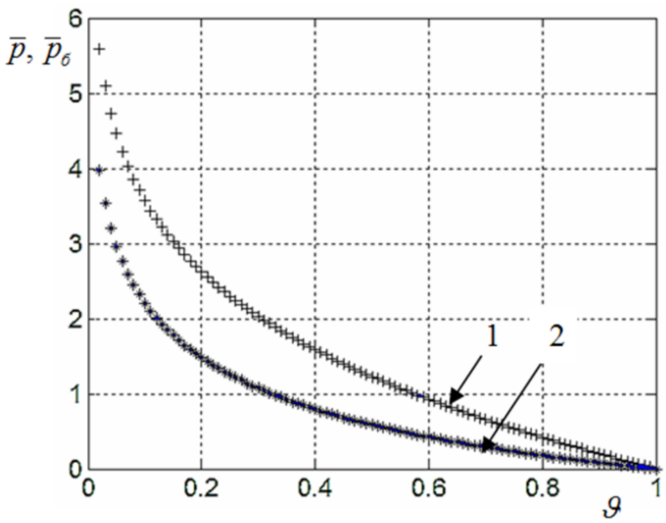

Fig. 6. Dependence of the plastic flow load $\bar{p}$ and side pressure $\bar{p}_b$ on the a pressing tool on the porosity ϑ of the compacted medium:

1 – $\bar{p}(\vartheta)$; *2* – $\bar{p}_b(\vartheta)$

Physical equations (3), and (4) were used to calculate the lateral pressure on the mold. The equation for calculating the lateral pressure has the following form

$$\bar{p}_b = \frac{p_b}{\tau_s} = \frac{1}{\sqrt{3}}(-1 + \vartheta^{2/3} - 2\ln\vartheta). \qquad (8)$$

The calculation results of $\bar{p}(\vartheta)$ and $\bar{p}_b(\vartheta)$ are shown in fig. 6.

Consider the stage of the *ECAP* process, in which the blank in the mold channel moves as a rigid plastic body. In this case, the deformation of the plastically compressible medium shape and volume changes is localized in the severe deformation layer (layer A-B). The layer thickness is $\Delta h \to 0$; the layer material is in a uniformly deformed state, which in the local coordinate system (n, τ, ς) can be represented by linear functions.

Following the kinematically admissible scheme of the flow of a plastically compressible medium for layer A-B, taking into account the boundary conditions, the velocity field is represented in the form:

$$[V^n] = |V_1 - V_2| \sin\alpha, \quad [V^\tau] = |V_1 + V_2| \cos\alpha, \ [V^\varsigma] = 0 \tag{9}$$

where $[V^i]$ is a spike of the velocity vector of material particles moving through the severe deformation layer.

The velocities V_1^n, V_2^n (fig. 3b) are connected by the condition of mass conservation:

$$V_1^n c_1 = V_2^n c_2; \ V_2 = V_1 \frac{1-\vartheta_1}{1-\vartheta_2}, \tag{10}$$

where ρ_1, ρ_2 is the density of the pressed material in parts II and I of the mold channel; ϑ_1, ϑ_2 is the porosity of the pressed material.

In the case of a plastically compressible medium, the system of equations also includes the continuity condition, which in [32] is reintegrated along the trajectory of the representative element of the volume. It follows from the mass conservation condition (10) that the intersection of the plastically compressible medium layer A-B leads to a change in the relative porosity of the medium. Taking into account the mass conservation condition and the continuity condition, the density of the extruded material from the mold channel is determined as:

$$c_2 = c_1 \exp \frac{2|V_1 - V_2|}{|V_1 + V_2|}. \tag{11}$$

Assuming that the relative density ρ of the compacted material is known from the analysis of the first stage of the *ECAP* process, the dissipation power of the severe deformation layer is calculated:

$$W|AB = \lim_{dh \to 0} (TH + \sigma\xi) S_{AB} dh. \tag{12}$$

The intensity of the shear deformation rate *H* and the deformation rate of change in the volume ξ of the A-B layer are determined by the following relations:

$$H = \frac{1}{dh}\left([V^\tau]^2 + \frac{4}{3}[V^n]^2\right)^{1/2}; \quad \xi = \frac{[V^n]}{dh}.$$

The power balance equation (2), in which the value $W|AB$ is calculated using equation (12), is applied to determine the energy-power parameters of the second stage of *ECAP*. Dividing the dissipative functions of the power balance equation by the values τ_s, V_1, $\pi D^2/4$ equation (2) results in a dimensionless form:

$$\bar{p}_1 = \bar{p}_2\chi + 4\left(k_1 \frac{L_1}{D} + k_2 \frac{L_2}{D}\chi\right) + \left(\sqrt{\frac{4}{3} + \left(\frac{1+\chi}{1-\chi}\cot(\alpha)\right)^2} - \frac{2}{\sqrt{3}} \frac{\ln(1-\rho)}{1-(1-\rho)^{2/3}}\right)(1-\chi) \tag{13}$$

$$k_1 = \frac{\tau_{c1}}{\tau_s^*}, \ k_2 = \frac{\tau_{c2}}{\tau_c^*}; \chi = \frac{V_2}{V_1}$$

where k_1, k_2 are coefficients in the *Siebel* friction law; $\chi = \rho_1 / \rho_2$ is the parameter characterizing the compaction of the compressible medium in the A-B layer.

Equation (13) is solved by the method of successive approximations. It is assumed that the density of the extruded blank is calculated for the previous stage of the studied process. The system of equations (1)–(13) makes it possible to unambiguously predict a set of technological parameters from cycle to cycle, which are necessary for the analysis and improvement of the *ECAP* process.

A series of computational experiments were performed to determine the effect of the angle α on the extrusion pressure $\bar{p}_1$ and the relative density of the extruded blank.

Calculations were performed for the following source data: $\vartheta_b = 0.4$; $L_1/D = 4$, $L_2/D = 2$; $k_1 = k_2 = 0.2$; $\chi = 0.8$; $\pi/16 \le \alpha \le \pi/2$. The values of density ρ and porosity ϑ of a plastically compressible blank at varying specific pressures $\bar{p}_1$ on the working plunger were determined using formulas (4), and (6). As a result, the dependence of pressing pressure $\bar{p}_1(\alpha)$ and blank porosity $\vartheta(\alpha)$ on the angle α (fig. 7) was determined.

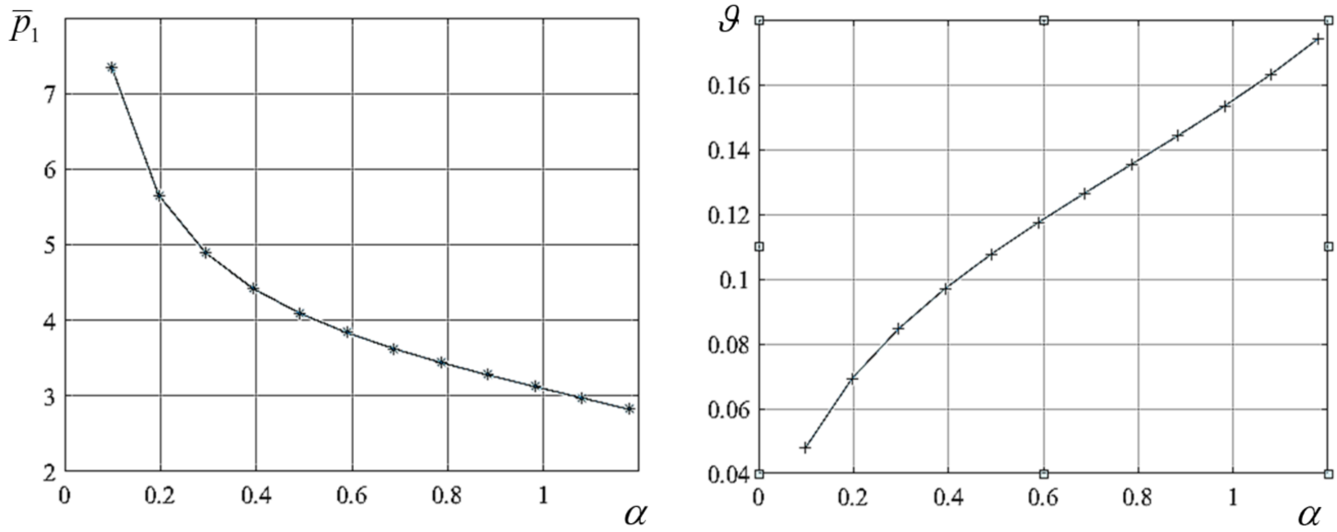

a *b*

Fig. 7. The dependence of the pressing pressure $\bar{p}_1$(б) (*a*) and porosity of the workpiece ϑ(б) (*b*) on the angle α

Numerical simulation of the *ECAP* process requires the use of a porous material plastic flow model included in modern *CAD* software. The simulation results significantly depend on the choice of both the material model itself and the methods of its identification. The *Gurson* model of plasticity of porous metal was used in this paper to describe the rheological behavior of the porous material [33]. The peculiarity of this model, implemented in the *Simulia/Abaqus FEA software package*, is the ability to describe the processes of both compaction and decompaction of powder materials in a wide range of stress-strain state changes. In this case, such a formulation of the problem makes it possible to identify areas of the deformable porous blank with a high level of tensile stresses during *ECAP*, and, therefore, potentially dangerous for the formation of surface cracks and material fracture. The following shows the application of the methodology for identifying porous titanium sponge blank plastic flow model.

Simulation modeling of the *ECAP* process was performed by the finite element method. The problem was solved in the volumetric formulation, but half of the section was used due to symmetry. For modeling, the *Explicit CAE calculation module* of the *Abaqus system* was used. A model of porous metal plasticity based on *Gurson's* theory of porous metal plasticity was used. The initial relative density was 0.6. The tool was set as absolutely rigid. The contact interaction between the blank and the tool was described by the *Amanton-Coulomb* friction condition, friction coefficient $\mu = 0.1$. It is assumed that the tangential stresses at the contact surface of the blank and tool are limited to $\tau_s = 30$ MPa.

Simulation using the finite element method makes it possible to estimate many parameters. In this case, it was limited to analyzing of the distribution of stress intensity σ_i and relative porosity ϑ, which is shown in figs. 8 and 9.

Fig. 8 shows the stress intensity distribution in the thin layer located in the vicinity of the section separating the inlet ***I*** and outlet ***II*** parts of the mold channel. It can be seen that the highest level of stress occurs during equal-channel angle pressing at α = 45°. The ratio of maximum stress intensity values between *ECAP* schemes with angles of 45 and 60° is 1.57.

The distribution of relative density across the section is most uniform when the angle α is 45° (fig. 9, *a*). At α = 50° porosity is detected only at the end of the blank, even though there is a counter-pressure. In other cases, there is decompaction in the contact zone of the blank with the surface of the mold channel.

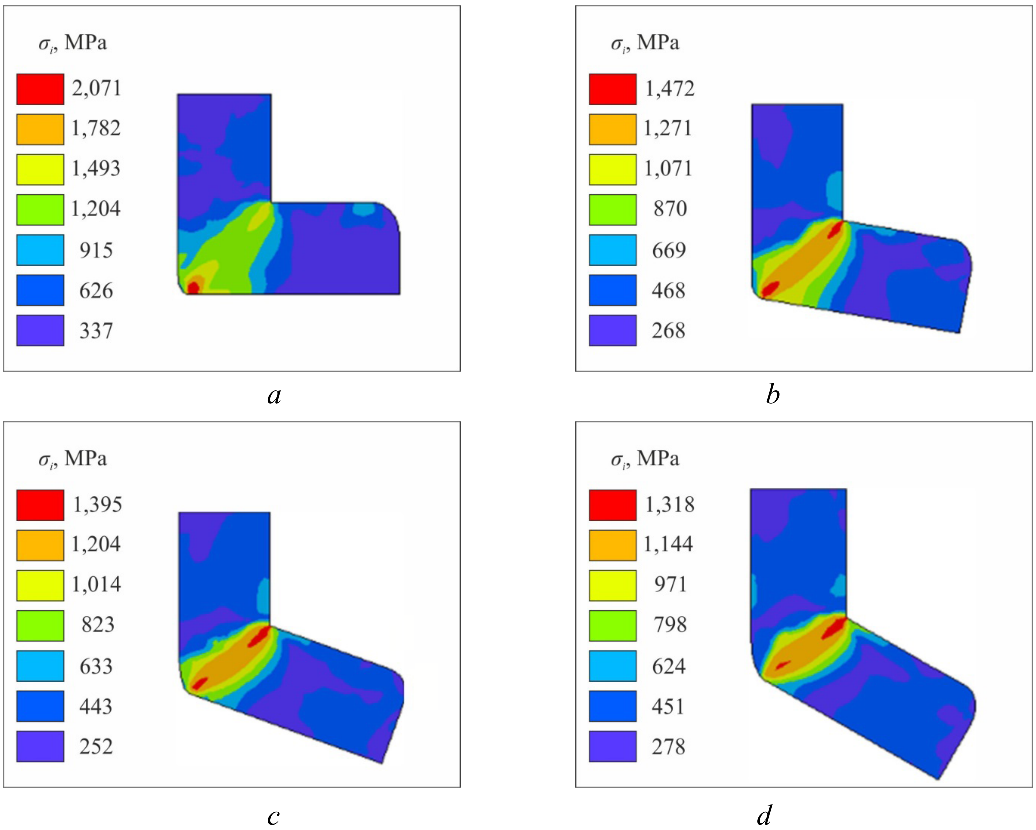

Fig. 8. The distribution of the yield stress σ_i at the steady stage of the process:
$\alpha = 45°$ (*a*); $\beta = 50°$ (*b*); $\alpha = 55°$ (*c*); $\alpha = 60°$ (*d*)

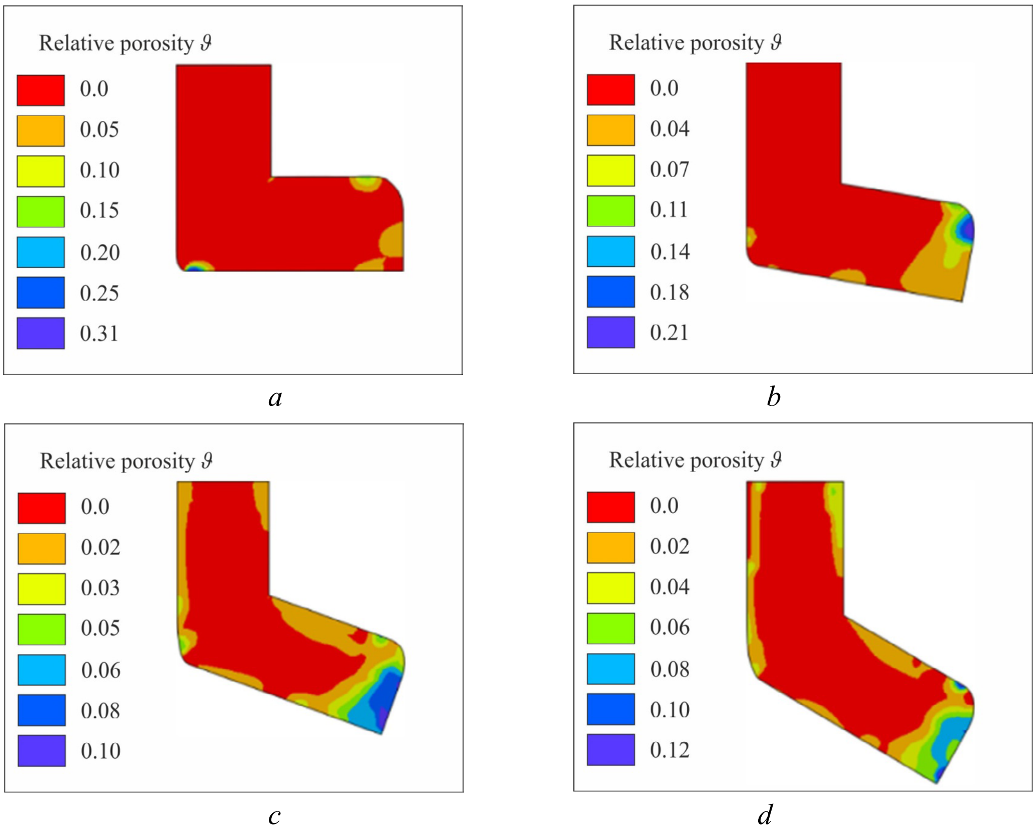

Fig. 9. Distribution of relative porosity ϑ at the steady stage of the process:
$\alpha = 45°$ (*a*); $\beta = 50°$ (*b*); $\alpha = 55°$ (*c*); $\alpha = 60°$ (*d*)

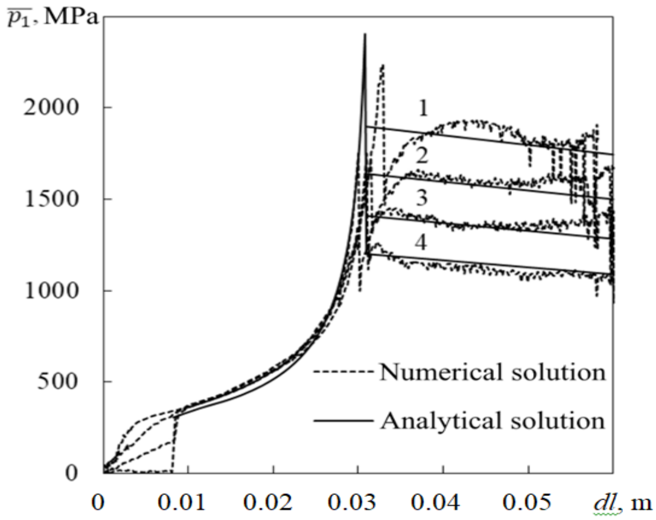

Fig. 10. The dependence of the pressing force $\overline{p}_1$ on the movement *dl* of the punch:
α = 45° (*1*); β = 50° (*2*); α = 55° (*3*); α = 60° (*4*)

In this case, the increase in the value of the relative porosity ϑ does not exceed 0.05. There is also considerable heterogeneity in the end region of the blanks.

The plot of pressure changes on the working plunger is shown in fig. 10.

The analytical calculations are performed following the results of the mathematical model, and the results of the numerical solution are obtained by computer simulation using the finite element method. The figure shows the satisfactory convergence of the solution results. The plot shows the variation of the compacting pressure at the main stages of the process. In the transition from the initial to the final stages of the *ECAP* process, the compacting pressure takes the maximum value. As the angle α increases, the maximum pressure on the working plunger decreases. During the transition from the initial stage of the *ECAP* process to the final stage, the pressing pressure takes on a maximum value [34–35]. As the angle α increases, the maximum pressure value on the working plunger decreases. Rational technological parameters of pressing porous blanks should provide the maximum permissible pressures on the deforming tool. From this condition, the optimal value of the angle in each specific *ECAP* process is determined 2α.

Conclusions

To optimize technological processes of manufacturing blanks and products from powders and porous materials, a sufficiently reliable and simple for practical use mathematical model of the process of semicontinuous *ECAP* of a plastically compressible medium is developed. The material properties of porous briquettes made by compacting titanium sponge in a closed mold were taken as a model material of initial blanks for the implementation of the studied process. The main stages of *ECAP* are considered: the initial stage of the process, in which the porous deformable material experiences compression in a closed mold; the stage characterized by intense plastic deformation localized by changing the mold channel angle; the final stage in which the deformable material is compressed to a nearly compact state and flows out of the mold channel as a solid body. The mathematical model makes it possible to determine the energy-power parameters of the *ECAP* process. In addition to the analytical solution, a finite-element simulation of the *ECAP* of porous material for a more detailed prediction of porosity along the blank cross section is given. A satisfactory correspondence of the results of calculating the energy-power parameters of the process is shown. The possibility of describing the processes of both compaction and decompaction of materials at the macro level in a wide range of volume plastic deformation will make it possible to more accurately determine the areas of the deformed porous blank subject to high tensile stresses during *ECAP*, which are potentially dangerous in terms of surface cracks formation and material fracture.

References

1. Zhilyaev A.P., Nurislamova G.V., Kim B.K., Baro M.D., Szpunar J.A., Langdon T.G. Experimental parameters influencing grain refinement and microstructural evolution during high-pressure torsion. *Acta Materialia*, 2003, vol. 51, iss. 3, pp. 753–765. DOI: 10.1016/S1359-6454(02)00466-4.

2. Saito Y., Utsunomiya H., Tsuji N., Sakai T. Novel ultra-high straining process for bulk materials – development of the accumulative roll-bonding (ARB) process. *Acta Materialia*, 1999, vol. 47, iss. 2, pp. 579–583. DOI: 10.1016/S1359-6454(98)00365-6.

3. Zherebtsov S.V., Salishchev G.A., Galeyeva R.M., Valiakhmetova O.R., Mironova S.Yu., Semiatin S.L. Production of submicrocrystalline structure in large-scale Ti–6Al–4V billet by warm severe deformation processing. *Scripta Materialia*, 2004, vol. 51, pp. 1147–1151. DOI: 10.1016/j.scriptamat.2004.08.018.

4. Richert M., Stuwe H.P., Zehetbauer M.J., Richert J., Pippan R., Motz Ch., Schafler E. Work hardening and microstructure of AlMg5 after severe plastic deformation by cyclic extrusion and compression. *Materials Science and Engineering: A.*, 2003, vol. 355, iss. 1–2, pp. 180–185. DOI: 10.1016/S0921-5093(03)00046-7.

5. Mani B., Jahedi M., Paydar M.H. Consolidation of commercial pure aluminum powder by torsional-equal channel angular pressing (T-ECAP) at room temperature. *Powder Technology*, 2012, vol. 219, pp. 1–8. DOI: 10.1016/j.powtec.2011.11.034.

6. Valiev R.Z., Estrin Yu., Horita Z., Langdon T.G., Zehetbauer M.J., Zhu Y.T. Producing bulk ultrafine-grained materials by severe plastic deformation. *JOM*, 2006, vol. 58, pp. 33–39. DOI: 10.1007/s11837-006-0213-7.

7. Segal V. Review: modes and processes of severe plastic deformation (SPD). *Materials*, 2018, vol. 11 (7), p. 1175. DOI: 10.3390/ma11071175.

8. William G., Voorkes J. Conform and Linex – continuous aluminium extrusion machines. *Light Metal Age*, 1978, vol. 36, iss. 1–2, pp. 18–20.

9. Thomas B.M., Derguti F., Jackson M. Continuous extrusion of a commercially pure titanium powder via the Conform process. *Materials Science and Technology*, 2017, vol. 33, iss. 7, pp. 899–903. DOI: 10.1080/02670836.2016.1245256.

10. Segal V.M. Mechanics of continuous equal-channel angular extrusion. *Journal of Materials Processing Technology*, 2010, vol. 210, pp. 542–549. DOI: 10.1016/j.jmatprotec.2009.11.001.

11. Lapovok R., Tomus D., Bettles C. Shear deformation with imposed hydrostatic pressure for enhanced compaction of powder. *Scripta Materialia*, 2008, vol. 58, iss. 10, pp. 898–901. DOI: 10.1016/j.scriptamat.2008.01.010.

12. Qi Y., Contreras K.G., Jung H.D., Kim H.E., Lapovok R., Estrin Y. Ultrafine-grained porous titanium and porous titanium/magnesium composites fabricated by space holder-enabled severe plastic deformation. *Materials Science and Engineering: C*, 2016, vol. 59, pp. 754–765. DOI: 10.1016/j.msec.2015.10.070.

13. Matsuki K., Aida T., Takeuchi T., Kusui J., Yokoe K. Microstructural characteristics and superplastic-like behavior in aluminum powder alloy consolidated by equal-channel angular pressing. *Acta Materialia*, 2000, vol. 48, iss. 10, pp. 2625–2632. DOI: 10.1016/S1359-6454(00)00061-6.

14. Xia K., Wu X. Back pressure equal channel angular consolidation of pure Al particles. *Scripta Materialia*, 2005, vol. 53, iss. 11, pp. 1225–1229. DOI: 10.1016/j.scriptamat.2005.08.012.

15. Chen W., Yamamoto Y., Peter W.H., Gorti S.B., Sabau A.S., Clark M.B., Nunn S.D., Kiggans J.O., Blue C.A., Williams J.C., Fuller B., Akhtar K. Cold compaction study of Armstrong Process® Ti–6Al–4V powders. *Powder Technology*, 2011, vol. 212, iss. 2, pp. 194–199. DOI: 10.1016/j.powtec.2011.08.007.

16. Crowley G. How to extract low-cost titanium. *Advanced Materials and Processes*, 2003, vol. 161, iss. 11, pp. 25–27.

17. Chen G.Z., Fray D.J., Farthing T.W. Direct electrochemical reduction of titanium dioxide to titanium in molten calcium chloride. *Nature*, 2000, vol. 407, pp. 361–364. DOI: 10.1038/35030069.

18. Donaldson A., Cordes R.A. Rapid plasma quenching for the production of ultrafine metal and ceramic powders. *JOM*, 2005, vol. 57, iss. 4, pp. 58–63. DOI: 10.1007/s11837-005-0083-4.

19. Ratnikov V.I., Prokudina V.K., Belikova A.F., Sachkova N.V. Obtaining of titanium powder from titanium sponge by self-propagating high-temperature synthesis hydration and dehydration. *Russian Journal of Non-Ferrous Metals*, 2010, vol. 51, iss. 4, pp. 352–358. DOI: 10.3103/S1067821210040176.

20. Bukhvalov A.B., Gorshkov M.M., Litvinov B.V. Effect of hydrogenation and hot-cold rolling of compact from titanium sponge on its structure, strain hardening, and fracture behavior. *Metal Science and Heat Treatment*, 2004, vol. 46, iss. 11–12, pp. 527–534. DOI: 10.1007/s11041-005-0013-7.

21. Rubshtein A.P., Trakhtenberg I.Sh., Makarova E.B., Triphonova E.B., Bliznets D.G., Yakovenkova L.I., Vladimirov A.B. Porous material based on spongy titanium granules: structure, mechanical properties, and osseointegration. *Materials Science and Engineering: C*, 2014, vol. 35, pp. 363–369. DOI: 10.1016/j.msec.2013.11.020.

22. Hadadzadeh A., Whitney M.A., Wells M.A., Corbin S.F. Analysis of compressibility behavior and development of a plastic yield model for uniaxial die compaction of sponge titanium powder. *Journal of Materials Processing Technology*, 2017, vol. 243, pp. 92–99. DOI: 10.1016/j.jmatprotec.2016.12.004.

23. Nesterenko A.V., Novozhonov V.I., Zalazinskii A.G., Skripov A.V. Vliyanie temperatury na kompaktiruemost' briketov iz titanovoi gubki, legirovannoi vodorodom [Influence of temperature on compactibility of briquettes

of titanium sponge alloyed with hydrogen]. *Izvestiya vysshikh uchebnykh zavedenii. Tsvetnaya metallurgiya = Izvestiya. Non-Ferrous Metallurgy*, 2015, no. 2, pp. 52–57. DOI: 10.17073/0021-3438-2015-2-52-57.

24. Nesterenko A.V., Novozhonov V.I., Vichuzhanin D.I. Vliyanie deformatsionnoi obrabotki na svoistva i strukturu polufabrikatov, poluchennykh tverdofaznoi konsolidatsiei titanovoi gubki [Influence of deformation treatment on the properties and structure of semi-finished products by solid-phase consolidation of titanium sponge]. *Izvestiya vysshikh uchebnykh zavedenii. Tsvetnaya metallurgiya = Izvestiya. Non-Ferrous Metallurgy*, 2015, no. 4, pp. 42–47. DOI: 10.17073/0021-3438-2015-4-42-47.

25. Nesterenko A.V., Novozhonov V.I., Zalazinsky A.G. Effect of deformation processing on the properties and structure of titanium obtained by plastic deformation of hydrogen-alloyed titanium sponge. *Diagnostics, Resource and Mechanics of materials and structures*, 2015, iss. 3, pp. 98–108. DOI: 10.17804/2410-9908.2015.3.098-108. (In Russian).

26. Berezin I.M., Zalazinskij A.G. *Press-forma dlya dvukhstoronnego pressovaniya poroshka* [Mold for double-sided pressing of powder]. Patent RF, no. 2686436, 2019.

27. Mitin B.S., ed. *Poroshkovaya metallurgiya i napylennye pokrytiya* [Powder metallurgy and sprayed coatings]. Moscow, Metallurgiya Publ., 1987. 792 p.

28. Kolmogorov V.L. *Napryazheniya. Deformatsii. Razrushenie* [Stresses. Deformations. Destruction]. Moscow, Metallurgiya Publ., 1970. 229 p.

29. Druyanov B.A. *Prikladnaya teoriya plastichnosti poristykh tel* [Applied theory of plasticity of porous bodies]. Moscow, Mashinostroenie Publ., 1989. 165 p.

30. Zalazinsky A.G., Kolmykov V.L., Sokolov M.V. O fizicheskikh uravneniyakh poristogo materiala [On the physical equations of a porous material]. *Izvestiya vuzov. Tsvetnaya Metallurgiya = Izvestiya. Non-Ferrous Metallurgy*, 1997, no. 4, pp. 39–43.

31. Zalazinsky A.G. *Plasticheskoe deformirovanie strukturno-neodnorodnykh materialov* [Plastic deformation of structurally inhomogeneous materials]. Yekaterinburg, IES UB RAS Publ., 2000. 492 p.

32. Zalazinsky A.G., Polyakov A.P. Postroenie razryvnogo resheniya dlya protsessa vydavlivaniya plasticheski szhimaemogo tela [Construction of a discontinuous solution for the process of extrusion of a plastically compressible body]. *Izvestiya vuzov. Mashinostroenie = BMSTU Journal of Mechanical Engineering*, 2001, no. 4, pp. 43–53.

33. Gurson A.L. Continuum theory of ductile rupture by void nucleation and growth: Pt. I. Yield criteria and flow rules for porous ductile materials. *Journal of Engineering Materials and Technology*, 1977, vol. 99, pp. 2–15.

34. Nagasekhar A.V., Tick-Hon Y., Li S., Seow H.P. Effect of acute tool-angles on equal channel angular extrusion/pressing. *Materials Science and Engineering: A*, 2005, vol. 410–411, pp. 269–272. DOI: 10.1016/j.msea.2005.08.043.

35. Li S., Bourke M.A.M., Beyerlein I.J., Alexander D.J., Clausen B. Finite element analysis of the plastic deformation zone and working load in equal channel angular extrusion. *Materials Science and Engineering: A*, 2004, vol. 382, iss. 1–2, pp. 217–236. DOI: 10.1016/j.msea.2004.04.067.

Conflicts of Interest

The authors declare no conflict of interest.